

# Investigation of a Low-Energy X-ray Spectrometer based on Pixellated Hybrid Silicon Detectors

P. Seller  
Rutherford Appleton Laboratory

2/4/2004

## 1.0 Background

RAL SSTD has the funding to propose a UK bid, named MIXS, for an X-ray Spectrometer instrument for the ESA, Horizon 2000, Cornerstone, BepiColombo mission to Mercury. BepiColombo consists of a lander element payload, a magnetospheric measurement satellite and a low altitude orbiter on which the X-ray Spectrometer will fly. It will be launched in 2012 and take 2.5 years to get to Mercury orbit for its 1 year operation.

DCIXS is a demonstrator spectrometer comprising a Swept Charge CCD device to be sent to the Moon. The Swept charge device is proving too radiation soft for the Mercury mission hence the investigation of Hybrid Silicon detectors.

There is a proposal based on MCP optics with Hybrid GaAs (40um thick) detectors. There is a 32x32 pixel 300um pitch ROIC being developed for this. There is also a proposed wider angle collimator design. There could be backups of both the ROIC and the GaAs detector. These could have a different pitch and also the detector material could be silicon. We have baselined a 30mm x 30mm detector plane but this will depend on many science and technical decisions.

NASA has a separate Mercury mission: Discovery Mission, Messenger, (MErcury Surface Space ENvironment GEOchemistry and Ranging), X-ray Spectrometer launching in 2005. This will be the first investigation of Mercury since the three Mariner flybys of 1975. It uses three poor resolution gas detectors with two filters to give spectroscopic measurements. Their detectors are developments of Apollo and NEAR detectors.

## 2.0 Measurements

The X-ray emission from the Hermian surface is due to X-Ray Fluorescence (XRF) most of the time but due to Particle Induced X-ray Emission (PIXE) during active solar particle emission phases. CIXS will measure primarily XRF. The emissions are at the characteristic  $K\alpha$  photo peaks of the surface elements; Mg(1.254keV), Al(1.487), Si(1.74), S(2.308), Ca(3.691), Ti(4.508), Fe(6.403). There are also Fe and O lines at about 700eV that might be of interest. All these should be resolved in the measured spectrum, which will require 200eV FWHM resolution from 500eV to 7keV. The square pores of a Micro Channel Plate Optic will be used to focus the X-rays onto the 3cm x 3cm active focal plane array 1m away. The X-ray photon rate is only 10-100Hz. Be or B filters will be used to reduce heat load but there will be considerable heating of the detector that requires heat extraction from the back of the detector module. During some of the 2.5year transit time the spectrometer could be activated for X-ray measurements

## 3.0 Apology

The intention of this paper is to present the feasibility of Hybrid Silicon Detectors for this application, not to compare this technology to Gaseous Detectors, Silicon Drift Detector, CCDs, Si(Li), Silicon Surface Barrier or other X-ray spectroscopy detectors. The later part of the paper does briefly compare the pixellated Silicon solution to a similar pixellated GaAs detector that has been proposed for similar missions.

## 4.0 Hybrid Silicon Detector

### 4.1 General construction and operation

The detector consists of a single piece of high-resistivity n type Silicon. The surface of the detector is patterned with individual implants and connection pads of Aluminium. These are bump bonded to an array of preamplifiers on an ASIC.

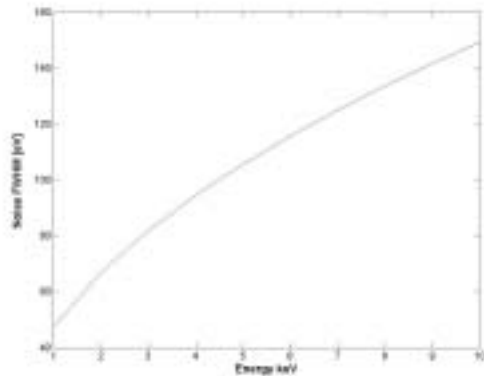
An X-ray entering the silicon will convert at a Silicon atom by Photoelectric emission of an energetic Photoelectron. The energetic electron in turn will lose energy by creating electron-hole pairs within a small distance. An Auger electron or characteristic Silicon fluorescence photon at 1.8keV will also be produced as the energy level in the Silicon atom is filled. These will quickly be absorbed and also be converted into electron-hole pairs. All the carriers will drift in the field in the detector and the holes will be collected at the preamplifier pads.

The mean energy to create an e-h pair in this process in Silicon is 3.66eV. Thus a 500eV photon will produce 140 charge carriers at the preamplifier and a 10keV photon produce 2800 charge carriers.

One might expect the statistical noise on the production of n charge carriers to be SQRT(n). Fortunately because of the process outlined above the statistics are better than this. The statistical noise of the conversion in a room temperature semiconductor is

$$ENC[FWHMeV] = 2.35\sqrt{\epsilon FE}$$

Where  $\epsilon$  is 3.66 in Silicon and F is the Fano factor which is about 0.12 in Silicon for all energies down to 600eV [1]. E is the energy of the X-ray. This noise is the best that can be done with this type of so called room temperature semiconductor detector. This fundamental resolution possible is plotted.



The limit is 45eV FWHM at 1keV rising to 143eV FWHM at 10keV.

#### 4.2 Silicon detector

Conventionally the irradiated side of the detector has an Ohmic contact for the positive bias. This usually consists of an n+ Phosphorous or Arsenic implant/diffusion with a thin Aluminium contact layer. The reverse side has the structured p+ Boron implantations for the individual pixel readouts. The detector is reverse biased so that the full thickness of the detector is depleted. This typically takes 50V for a 300um thick detector. The field thus produced in the depleted region drifts any charge carriers to the contacts (holes to the p+ contacts). We will discuss later the profile of this drift process and the associated charge sharing between pixels due to competing lateral diffusion.

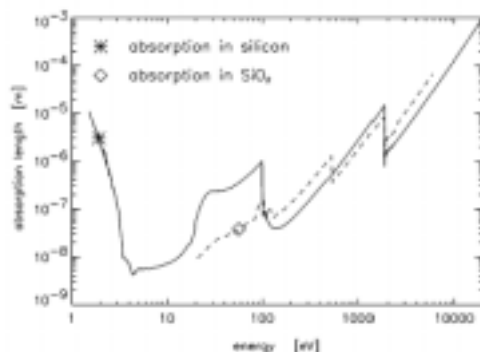
For other semiconductor detector materials incomplete collection of charge from the depletion region is a significant problem; but with the envisioned thickness of Silicon we can neglect this process.

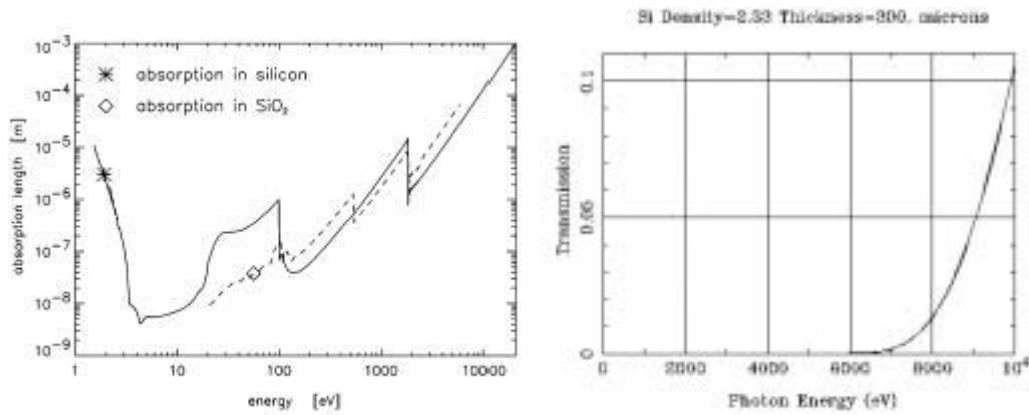
Leakage current is a problem. The current is thermally generated in the bulk and also injected from the contacts. Excess leakage is generated by mid gap states. In the very good quality detector material now available contamination is less of a problem but a good defect gettering layer on the irradiated side can significantly improve the performance. This is supplied by the Phosphorous n+ doping.

Surface properties on the pixel side can cause low inter-pixel resistance, which in turn causes poor performance. This is predominantly due to surface charge and high surface fields. This can be completely overcome in our geometries with oxide passivation and adequate design of guard band structures around the outside of the detector. Problems do exist in this area but primarily with polyimide passivation and very high over-voltaged detectors which we will avoid in this detector.

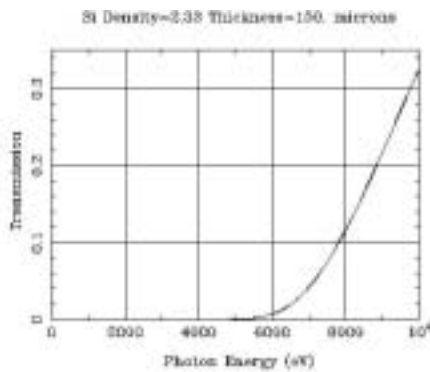
##### 4.2.1 High energy cut off

The absorption depth in Silicon for different energies of X-rays is plotted here.





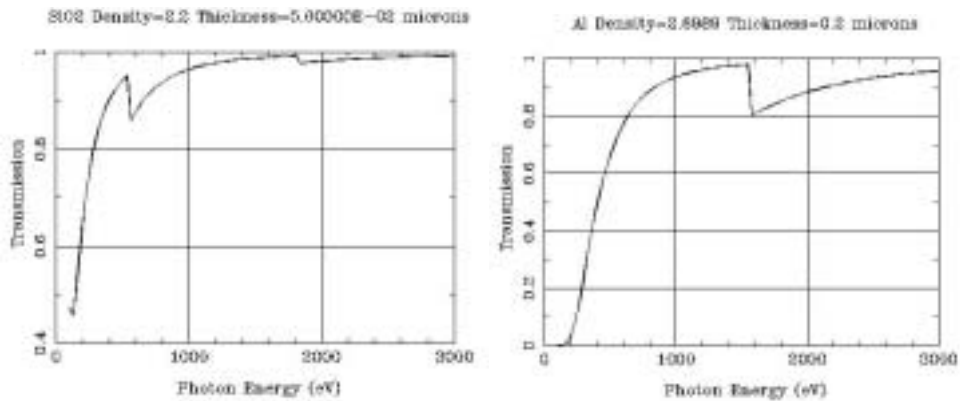
As can be seen all X-rays up to 10keV will be stopped by 300um of Silicon with 90% efficiency. 300um is a standard thickness of wafers. The advantages of reducing this thickness are to reduce the depletion voltage, reduce the leakage current but in our application the most significant effect might be to reduce large amplitude background hits. This only reduces linearly with thickness. Below 150um the mechanical strength during bump bonding starts to be a problem. Also there may be mechanically induced leakage current generated. The efficiency for 150um thick Si is shown here.



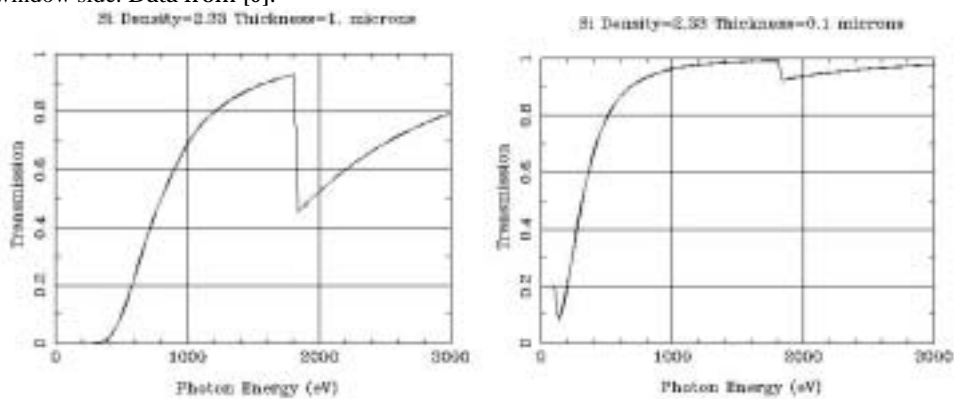
#### 4.2.2 Low energy cut off

This issue is one of the principal research elements required for this detector in this application. Surface barrier [2] and Si(Li) [3] detectors have been used for low-energy X-ray and alpha detection but are cryogenic detectors and are unsuitable for this application. The deep depleted p-n CCD and Silicon Drift Detectors are built on high resistivity n- material identical to our silicon pixel detectors [4], [5] as well as [6] and [7]. They however use p+ rectifying contacts on the back and front, only using small n+ contact for the signal collecting anode. This produces shallow diffusions but more importantly sharply defined high field regions that also reflect charge carriers that try to enter the low field region. Drift detectors have achieved good resolution down to 500eV and below. These are built with a p+ diffusion over-doped with an n+ diffusion to increase the local electric field. This approach has clearly succeeded. Hartmann [8] also reports better low-energy performance with  $\langle 111 \rangle$  material rather than  $\langle 100 \rangle$  due to reduced channelling of implants

Low energy X-rays of 100eV-3keV have very short absorption lengths in Aluminium, Silicon Dioxide and Silicon as shown in the expanded plot. A detector could be built with the window side lightly oxidised and have a ring of Al around the active area; in this case we might have 50nm of oxide on the Si. It is also possible to have 200nm of Al on the surface for good contact to the diffusion. These options are presented here.



With a thick inactive n+ Phosphorous diffusion of 1um the graph shows an appreciable attenuation around 1keV and at 2keV. The situation is much better at 100nm dead layer as in the shallow p+ rectifying contact on the window side. Data from [9].



It is clear from this that to achieve good quantum efficiency and energy performance at 1keV we must start with a contact below 1um thick. Typical Silicon pixel detectors have n+ Ohmic contacts on the irradiated side of the detector consisting of 200nm of Aluminium with 1um depth of Phosphorous implantation in to the Silicon. If X-rays convert in the Aluminium or n+ implant they produce ionisation but as it is not in a field it recombines and is not seen in our signal current. This is most important with low energy photons <3keV.

For X-rays above the K edge of Silicon a fluorescence X-ray can be produced (4%) rather than an Auger electron. This 1.8keV photon has significant range (<12um) and can escape from the field region and be lost from the signal energy, giving the characteristic 'escape peak'. Nothing can be done about this effect which is seen in all semiconductor detectors. Photons below the K edge obviously excite only the L shell electrons in Silicon so no K escape peak is produced.

A more detailed study of the primary Photoelectron and Auger electron explains other problems in the low energy spectrum [10]. Both non-thermal electrons have short but significant ranges so that electrons produced in the zero field regions can enter the field regions and visa versa. This leads to partial collection of the X-ray energy and a distortion of the Gaussian Photopeak. This effect is compounded due to the implantation and diffusion profile of the n+ implant in the Silicon. This intermediately doped region produces a signal with only part of the signal current given in the detector and part of it recombining. These effects present themselves as a background level or shoulder below the Photo-peak, often grossly characterised as a peak to background ratio.

The low energy acceptance of the detector is clearly maximised by making the zero field regions as small as possible. This includes making the Al thin, eliminating any oxide layer and minimising the thickness of the window-side implanted/diffused region. This has to be done while maintaining low leakage current in the detector and acceptable robustness of the surface.

The effects from partial conversion of non-thermal electrons are minimised by making the diffusion profiles as sharp as possible. Lowe [11] reports on the mechanisms of low-energy spectral phenomenon produced by electron thermalisation at barriers.

#### 4.2.2.1 p+ pixel readout on n- material

Conventionally simple pixel detectors are built on n- material with an n+ Ohmic contact for the irradiated side. This contact would need development to optimise for thin zero-field region. Canberra has detector technology with thinned p+ contacts but can also thin the n+ Ohmic contact. Sintef has built thinned Phosphorous and Arsenic Ohmic contacts for the Impact work and still showed good leakage currents. The low energy performance of these detectors was not measured due to the limitations of the readout electronics available. It is proposed to measure the low energy performance of these detectors with different electronics.

One limitation of illuminating the n+ Ohmic contact side of the detector is that it has to be fully depleted and maybe slightly over depleted. This is because the depletion region starts growing from the p+ contact through the n- high-resistivity material with increasing voltage. The material next to the n+ contact will only deplete at full voltage and then drive slowly into the n+ layer. There will then have to be a trade-off between leakage current and zero-field thickness.

One possible compromise is to diffuse a deep n+ grid on a shallow n+ irradiated side contact. This will compromise the low energy acceptance less and hopefully would retain the good gettering properties. It is hard to see how to calculate these effects more accurately than a geometric approximation. Reliable data on performance and response would require a test structure.

#### 4.2.2.1 n+ pixel readout on n- material

Silicon Drift Detectors use p+ diffusions on the window as well as on the bonded side with a row of n+ contacts bonded to the electronic readout. Specialised High Energy Physics Detectors are also made with n+ contacts on n- material. In these detectors the n+ pixels are separated by p+ diffusions called channel stops, to ensure low inter-pixel resistance and to ensure separation of the pixels for charge carrier readout. These p+ diffusions on the bonded side are either a complete grid across the detector or isolated 'atolls' around each pixel. The advantage of this is that on the window side the p+ diffusions are thinner than n+ Ohmic contacts. Also the +ve voltage could tend to reflect the photoelectrons into the active region. Because the depletion region grows from the p+ interface into the n- material the window side active region will exist immediately reverse bias is applied. It also grows slowly into the p+ contact with increasing depletion voltage. The disadvantage is that the detector will have to be fully depleted before the pixels are well separated electrically. The inter-diffusion capacitance might be higher due to the smaller distances and there is reported concern about incomplete collection of charge. Also the detector is much more complicated to process as the bonded surface has n and p diffusions.

This detector might present the best solution in our application predominantly due to the possibility of the thin p+ diffusion on the window side allowing better low energy performance.

The likely manufacturers will be Sintef or Canberra. Canberra have specific low-energy processes with thin windows for instance their Alpha PIPS process shown in the table.

MODEL	A300	A450	A600	A900	A1200
Active Area (mm <sup>2</sup> )	300	450	600	900	1200
Active Diameter (mm)	19.5	23.9	27.6	33.9	39.1
Thickness (min/max $\mu$ )	150/315	150/315	150/315	150/315	150/315
Bias (min/max V)	+20/100	+20/100	+20/100	+20/100	+20/100
Bias (recommended V)	+20/80	+20/80	+20/80	+20/80	+20/80
Si-Resistivity (min ohm-cm)	2000	2000	2000	2000	2000
Operating Temp (min/max $^{\circ}$ C)	-20/+40	-20/+40	-20/+40	-20/+40	-20/+40
Storage Temp (max $^{\circ}$ C)	+100	+100	+100	+100	+100
Leakage current (typ/max) nanoamps at 25 $^{\circ}$ C <sup>1</sup>	35/70	50/100	60/120	100/200	150/300
Alpha Resolution <sup>2</sup> keV (FWHM)	17/19	18/20	23/25	25/30	30/37
Absolute Efficiency (%) <sup>3</sup>					
at 2 mm spacing	37	40	24	44	45
at 5 mm spacing	24	28	31	35	37
at 15 mm spacing	7	11	12	16	19

From this example we can see a leakage current of 120pA/mm<sup>2</sup> (12pA/pixel) for 150um material which is not really acceptable for our application. See the section on leakage current for more about this issue.

#### 4.2.3 Spectral resolution, signal tailing and artefacts

##### 4.2.3.1 Electronic noise

We have seen the Fano limit as the fundamental resolution of room temperature semiconductor detectors. This is not achieved primarily due to so called thermal noise of the preamplifier and the way the electronics deals with the detector leakage current. This leads to a Gaussian broadening of the photopeaks and will be covered in the section on electronics.

#### 4.2.3.2 Window side contact

The section on Low energy cut off describes the effect on spectral uniformity and peak-valley ratios produced by the contact on the irradiated side.

#### 4.2.3.3 Charge carrier loss

We ignore charge loss during transport in the bulk of the detector, as the Silicon material is very good in this respect even after irradiation.

#### 4.2.3.4 Escape peaks

As described previously in X-ray absorption a 1.8keV photon is produced when the excited Silicon atom decays. This has a yield of only 4% compared to the Auger electron production decay. If this occurs near a surface this energy can be lost from the signal value, leading to the so-called Silicon 'escape peaks'. This can be worse in pixellated detectors as the photon can leave its energy in adjacent pixels. Thus the escape peak magnitude can be greater than would be seen from a single element device of the same size. If the adjacent pixel energy is added back to the primary pixel energy this effect can be minimised.

#### 4.2.3.5 Charge sharing

The initial photo electron produce charge carriers in a sub-micron region. These carriers then start to diffuse. They are also being drifted in the field in the depleted region. This results in a net Gaussian distribution on the pixel side surface. The size of the image is dependant on the interaction depth of the photon. The higher the field, the faster the drift and the smaller the image. Typically the mean projected size is 20um. With 300um pixels this means 1% of events will share their signal over two pixels. Unless the pixel energies are summed this charge-sharing leads to energy loss for the event and thus a tailing in the spectrum.

### 4.2.4 Radiation hardness

#### 4.2.4.1 Proton

This is the major mechanism responsible for damage in silicon detectors. In CCDs this is responsible for reduced charge transfer efficiency as well as bulk damage. As pixellated detectors do not use the charge transfer technique this is not of concern. Protons do cause lattice damage in the bulk producing mid band states and thus increased leakage current. Struder [12] reports measurements on 285um n- type material of  $1.2-2.5 \times 10^{-16}$  A/p reducing after annealing to  $0.7-1.5 \times 10^{-16}$  A/p with 10MeV protons.

This damage coefficient is presented in another way in the High-Energy Physics community such as Lemeilleur [13], who gives  $1 \times 10^{-17}$  A/cm<sup>3</sup> per fluence [p/cm<sup>2</sup>] for irradiation with 24GeV/c protons. This is  $1 \times 10^{-17}$  A/p-cm, which gives  $3 \times 10^{-16}$  A/p for a 300um thick detector, which is a roughly comparable result.

In our case with 150um thick detectors, the damage is half the 285um detector case. So this gives a worst case increase in leakage current of  $1 \times 10^{-16}$  A/p.

We require a leakage of only 2pA/pixel or 2nA/cm<sup>2</sup> and if we assume all this comes from damage we then could only stand  $2 \times 10^7$  p/cm<sup>2</sup> for the life of the mission.

Struder anticipated [14] a fluence over the 10 year life for XMM of  $4 \times 10^8$  p/cm<sup>2</sup>. We could assume this for a shorter mission but in a more aggressive environment. This is clearly an unacceptable increase from our 2pA/pixel requirement to 40pA/pixel.

Smart 1 reports a simulated reduction of four orders of magnitude in ionising radiation using 5mm of Aluminium [15]. They are then predicting 20kRads of ionising radiation for the mission behind the shielding which would be acceptable for the silicon damage. The Non Ionising Energy Lose equivalent to 10MeV proton fluence is however very high. They predict  $7 \times 10^{15}$  p/cm<sup>2</sup> from trapped protons and  $4 \times 10^{12}$  p/cm<sup>2</sup> from solar protons. While we will not see the mission dose from trapped protons as we escape earth orbit more quickly, we will see at least this level of solar protons. The obvious recourse is shielding. But even after 20mm of Aluminium there are still  $1 \times 10^9$  p/cm<sup>2</sup> or 100pA/pixel.

(The latest estimate is slightly higher at  $1.6 \times 10^{13}$  p/cm<sup>2</sup> filtering to  $4 \times 10^9$  p/cm<sup>2</sup> or 400pA/pixel. In this case the only recourse is to cool; but even at -20C this would give 12pA.)

Oxygenated Silicon has been proposed to increase hardness [16] but seems to be sensitive to the type of irradiation and more effective for severe ionising radiation doses than Non Ionising Energy Loss.

Annealing does offer further extension of life but if we use the silver loaded epoxy based Gold Stud bump bonding technique we will be limited to very modest 110C temperatures. Lead-tin solder bonding does offer higher temperature but we would not want to drive impurities into the detector or contaminate surface layers on the detector and electronics.

#### 4.2.4.2 X-rays

X-ray photons at these energies do not effect Silicon at all until they interact via the Photoelectric effect. The non-thermal electrons produced in this interaction can cause disruption to the Silicon lattice. Only 15-25ev is needed to produce lattice damage in Silicon but this requires very high-energy electrons of 200keV to have an appreciable cross section to deposit this energy. The effect in the bulk is to create mid gap states that increase leakage current.

A potential problem is with the pixellated back surface of the detector. Damage at this surface can cause surface charge leading to inversion of the silicon and low inter-pixel resistance. The detector itself protects this surface as most of the X-rays are absorbed in the detector material. Further shielding behind the detector as mentioned above will adequately protect the detector and electronics.

#### 4.2.5 Pixel capacitance

The capacitance of the pixel is important as it controls the possible noise performance of the detector. The capacitance has contributions from the parallel plate capacitance through the silicon volume but mostly from the inter-pixel capacitance. Measurements on similar detectors [17], [18] show that for a 300um square detector the capacitance will be roughly 200fF. This will increase to 300fF with interconnection to the readout chip.

#### 4.2.6 Leakage current

If we assume we will be able to hold the Silicon Detector to 20C then we could conservatively set the upper leakage-current acceptance level to a few pA/pixel or 20pA/mm<sup>2</sup>. For a typical p+ on n- detectors with thick Phosphorous n+ gettering layers there will be 10pA/mm<sup>2</sup> at 20C [19]. We have measured 160 pA/cm<sup>2</sup> for large diodes on 500um thick detectors from Sintef. This would equate to 0.15 pA/pixel of 300umx300um. We have measured single pixels of this size on 500um thick detectors from the same process and measured 0.3pA/pixel and this may be an upper limit due to the accuracy of our measurement equipment. This would definitely be acceptable. We have measured Canberra strip detectors with 18pA/mm<sup>2</sup> on 300um thick detectors at 20C. This would be just about acceptable and we would get less leakage if we went to 150um thick detectors. Also we could investigate the n+ grid on the ohmic side to improve low-energy acceptance. The detectors above had thick (1.5um) n+ layers on the window side. If we want thin p+ diffusions on the window side then we will have to look seriously at gettering [20]. The Canberra PIPS detectors for Alpha spectroscopy with thin p+ windows have 10 times more leakage than acceptable. A new idea might be to make the n+ contacts sufficiently large on the bonded side to give effective gettering [21], overcoming the problem of increased leakage current. The leakage current needs to be re-measured on the specific detectors with the illuminated side processing that has been selected for best low-energy efficiency. The leakage current will change with gettering performance of the n+ contacts and p+ stop geometry.

#### 4.2.7 Recommendation for detector geometry

We definitely need p+ contact on the window side to have thin diffusion for good low energy acceptance and to reflect Photo-electrons. In this case we will probably be struggling to achieve the leakage current requirements so we need to go to the small pixels of 300umx300um. We must also try the idea of thick n+ contact diffusions on the bonded side to see their gettering performance. We will use p+ stops in a continuous grid around the n+ pixels. It will be interesting to see if we can use a fan-in as used in Impact to give a continuously active 3cm x 3cm array with readout from the back.

## 5.0 Readout Electronics

### 5.1 Existing systems

There are several existing systems reported for readout of hybrid silicon detectors for low energy X-ray spectroscopy: The work at RAL for the Impact project has demonstrated 250eV FWHM resolution for Mn line (5.9keV) at room temperature with a 16x16 array of 300um square pixels. The low energy floor of the system is 5keV due probably to the comparator used in the readout system. The detector would almost certainly detect lower than this. Krieger [22], [23] reports a linear system with 180eV and an 8x8 pixel array with 210eV FWHM at -10C. This had 1mm pixels and dissipated 6mW per pixel. Again only measurement of Mn X-rays are reported. Pullia [24] has reported 165eV FWHM (-39C) and 320eV FWHM (26C) for a detector with 16 pixels of 1.5mm square. O'Connor [25], [26] reports the results of a linear system for SDD detectors with the equivalent electronic noise of 90eV FWHM. Misiakos [27] reports a 270um by 270um pixel with 300eV FWHM for low energy X-rays.

### 5.2 Overview of the advantage of detector segmentation

The noise when a signal charge from a detector is measured by the readout electronics is given by [28] as

$$ENC^2 = \left( \frac{b_t}{\tau} c_{tot}^2 kT \frac{2}{3gm} + b_s \bar{n} q + b_f c_{tot}^2 \frac{K_f}{WLC_{ox}} \right) [coulomb^2]$$

where

$$c_{tot} = c_d + c_{in} + c_f$$

The noise is given in terms of the Equivalent Noise Charge (sigma) that would be seen from the detector. The contributions are respectively from thermal noise in the pre-amplifier, leakage current from the detector and flicker noise in the pre-amplifier. There seem to be a lot of variables but we do not have much control over these. The coefficients  $b_t$ ,  $b_s$  and  $b_f$  are constants defined by the type of signal processing being used but do not change by more than a factor of 3. We can change the time constant  $\tau$ , of the filter to balance the contributions from thermal and leakage current but the major effect on the equation is to reduce  $c_{tot}$  and i.. This can be done by reducing the effective size of the detector seen by each pre-amplifier i.e. segmenting the detector.

**Splitting the readout of the detector into 100 pixels reduces the thermal and flicker noise by 100. As the leakage current is reduced by 100 times, the leakage current noise is reduced by a factor of 10. This is the rationale for a pixellated detector for this application. An added advantage is that the overall rate capability goes up but this is not a concern in this application.**

The competing constraints are obviously that there are more preamplifiers to readout which increases power, these have to be packed into a small pixel and the charge sharing issues in the detector become greater. These as well as the bonding technology have to be balanced against the advantages when optimising the pixel size. For instance a 300um x 300um pixel on a 300um detector will give 1-10pA and a capacitance of 300fF at 20C. A detector like this has been measured to give 250eV FWHM resolution.

### 5.3 Speed

The worst case overall rate on the detector is 100Hz. We may have 10 000 pixels. So the rate in any pixel is only 10milliHz. The shaping time in the pixel will thus be chosen to give the best noise. This very low rate will impact on the readout architecture.

### 5.4 Noise

As we have seen from section on detectors the Fano limit is 45eV FWHM at 1keV rising to 143eV FWHM at 10keV. This is equivalent to 5 electrons RMS to 17 electrons RMS. This has to be added in quadrature to the noise produced by electronic readout.

#### 5.4.1 Thermal noise

Assuming CR-RC shaping we have

$$ENC^2 = \left( \frac{3.7}{\tau} c_{tot}^2 kT \frac{2}{3gm} \right) [coulomb^2]$$

If we use a 0.25um process with a 80:0.35um PMOS input FET at 10uA drain current giving a gm of 0.25mS and a gate capacitance of 100fF. With 4us shaping and 300fF detector this gives 8 e- RMS or 68eV FWHM.

#### 5.4.2 Leakage current noise

Assuming CR-RC shaping we have

$$ENC^2 = (1.85\pi q) [coulomb^2]$$

With 4us shaping and 2pA leakage this gives 9 e- RMS or 80eV FWHM.

#### 5.4.3 Flicker noise

Assuming CR-RC shaping we have

$$ENC^2 = \left( 3.7 c_{tot}^2 \frac{K_f}{WLC_{ox}} \right) [coulomb^2]$$

If we use a 0.25um process with a 80:0.35um input PMOS FET with  $k_f=2e-25$  and  $c_{ox}=5fF/um^2$  this gives 6 e- RMS or 51eV FWHM.

#### 5.4.4 Total noise

Assuming CR-RC shaping and recasting the equation in terms of electrons RMS we have a total noise including the detector of

$$ENC^2 = \frac{1}{q^2} \left( \frac{3.7}{\tau} c_{tot}^2 kT \frac{2}{3gm} + 1.85\pi q + 3.7 c_{tot}^2 \frac{K_f}{WLC_{ox}} \right) + (DetectorFanoNoise)^2 [electrons^2]$$

$$ENC^2 = (64 + 81 + 36 + 25) [electrons^2] \text{ at 1keV}$$

$$ENC^2 = (64 + 81 + 36 + 289) \left[ \text{electrons}^2 \right] \text{ at } 10\text{keV}$$

This is 123eV FWHM at 1keV rising to 186eV FWHM at 10keV.

### 5.5 Pre-amplifier design

The preamplifier will be a folded cascode based charge amplifier with a small feedback (integrating capacitor). Due to the small size of the capacitor (approx. 10fF) there will be a detector leakage current compensation circuit. This will have to handle the 2pA leakage set as our acceptance criteria for the detectors. These techniques are reported by O'Connor [24 ], Pullia [23 ] etc..

### 5.6 Radiation hardness

In order to achieve the maximum performance and also the maximum future proofing of the design we will chose a 0.25um CMOS technology. These technologies have very thin gate oxides and are inherently radiation hard. Negligible parameter variations are seen after MGray of ionising radiation and large neutron dose. Also the devices can be effectively shielded by the substrate of the mounting and to a substantial level by the Silicon detector itself. This issue while important to address by device batch testing after construction is not seen as a major issue to be considered here.

### 5.7 Readout architecture

#### 5.7.1 Pre-amplifier, shaper and track-and-hold

The pre-amplifier will deliver a step voltage to the following circuit. Assuming a 10fF feedback capacitor this will be  $V=q/c$  or 4.4mV for a 1keV photon. This will have a droop rate because of the leakage current compensation that will probably be used rather than a switched reset. In order to reduce thermal noise we will shape the step with a CR-RC filter and amplify the signal by 20. This will filter the high frequency components and differentiate the long slope. The shaped signal will peak at around 4us as a compromise between reducing thermal noise and increasing leakage current noise. The peak value will be  $20/e$  of the step value so 32mV for a 1keV photon with a 2.5mV variance.

The output from the shaper will be held by a track-and-peak-hold circuit. This circuit has been used successfully in many ASICs. This circumvents time walk problems that have previously been overcome with power-hungry constant-fraction-discriminator circuits.

#### 5.7.2 Signal distribution and ADC

Let us assume a 3cm x 3cm array of 100 x 100 pixels. We will leverage technology developed in the Monolithic Active Pixel program at RAL. This work has been adapted here for the Hybrid Detector configuration.

The scheme uses a Row Select signal that synchronously latches all analogue outputs of a row onto 100 Column Outputs. It then quickly (<1us) resets the track-and-hold circuit but not the pre-amplifier or shaper. Each Column Output ends in one comparator and one latch of a distributed Wilkinson ADC, which converts to 10 bits in 1000 clocks. The ADC has one 10MHz-clock and ramp generator for each chip. The system can thus convert each row in 100us. The 100 x 10 bits are passed to Output Buffers and shifted out serially while the next row is being converted. At this rate the system can complete a whole frame readout in 10ms. This is a frame rate of 100Hz or an effective pixel rate of 1MHz. In our application we could readout at 10 Hz frame rate so an effective pixel rate of 100kHz. The dead time per pixel is 100us per frame so in the latter case  $100\text{us}/0.1\text{s} = 0.1\%$ .

A potential problem exists because the synchronous convert could convert during a 4us rise time of a signal. With 10 Hz signal rate this will happen  $4\text{us} \times 10/100\text{ms} = 0.04\%$  of the time. This is probably not a significant effect on the spectra but there is the capability to reject even this. We could reject signals that have two successive non-zero values. This will reject signals only partly developed on the track-and-hold circuit.

An even lower risk solution would be to have an ADC offchip and simply have signal multiplexers on board. A low power 9 or 10bit ADC working at 40kHz would suffice here and make the analogue array even simpler.

The attraction of this scheme is that the pixels are quite simple and there is only one digital control input. It is also very attractive not to have an analogue comparator in the pixel, as these are very difficult to set accurately in ASIC technology. Additionally there is only one 10-bit counter and ramp generator per chip allowing low extra power dissipation. The ADC and readout should be constrained to less than 400um allowing us to butt the readout chips very close. If the detector technology allows multiple levels of metal it may be possible to have no dead area on the 3cm x 3cm array.

We have chosen several of the parameters in order to make a low noise system. The 10MHz clock is well outside the  $1/(2\pi(4\mu\text{s}))=39\text{kHz}$  acceptance of the input filters ensuring a low level of clock feed-through. It is envisioned to use local power supply conditioning in each pixel and to run at a constant row readout rate of 1ms. Each row will take 100 $\mu\text{s}$  to readout.

### 5.7.3 Gamma and particle interactions

We expect numerous large energy depositions in the detector with a rate possibly in excess of the low-energy photons of interest. The rate is given by the flux interacting with the  $3\text{cm}\times 3\text{cm}\times 150\mu\text{m}=135\text{mm}^3$  silicon detector. We could assume 10MeV interactions at 100Hz. This would be equivalent to  $3.5\text{e}8\text{ p/cm}^2/\text{year}$  as used earlier in the radiation damage section.

10MeV gives  $5\text{e}-13\text{Coulombs}$  in the amplifier. With a leakage current compensation circuit capable of handling 100pA this would give a recovery time of 5ms. There are 10 000 pixels so the effective dead-time is 500ns. For the 100Hz rate this is 0.005% dead-time. A detailed design will have to be done to make sure that during time taken to restoring the pixel other photons hitting the pixel are not included in the spectra. This could potentially cause a lowering of these measured values.

Large charges applied to the pre-amplifiers can saturate the output stages that affect the power supply current drawn. This can then lead to cross talk to other pixels via the power supplies. This has been handled in other designs by output clamping. This will be addressed in the detailed design.

### 5.8 Power

The power from the pre-amplifiers is dominated by the input FET so should give 15uA per pixel. We then also have the leakage current compensation circuit. Without doing a detailed analysis it is not possible to be accurate but the shapers will contribute about the same, giving a total of 30uA to 40uA dissipation at 3.3V. As identified above the rest of the on chip electronics will contribute only a small increase on this 130uW.

If we assume 300um x 300um pixels and a 30mm x 30mm detector coverage this gives 10,000 pixels so would dissipate 1.3W for the whole array.

Over a small range of pixel size the power per pixel is independent of size assuming we could hold the leakage current to 2pA. At present the leakage is dominated by proton induced end-of-life leakage that to a large uncertainty could be constrained to 100pA at 20C. As a rule of thumb leakage reduces by a factor of 2 every 8C. Thus at -20C this could give 3pA.

Another possibility is that if the pixels were increased to 1mm x 1mm there would be only 900 pixels and then the power dissipation could possibly be reduced dramatically to 130mW. This is at the limit of the leakage current prediction and also it above this size the capacitance of the pixel increases with size and so other factors in the noise equation start increasing. Also the power to take the signal from the increased capacitance increases and a direct extrapolation no longer works.

## 6.0 Time-scales

### 6.1 Detector

Detectors take about 2months to design to take into account the CAD and test structure definition. They take typically 4 months to fabricate. The wafers are shipped with leakage current and C-V measurements that will confirm depletion but does not confirm they are working as good detectors. The further sawing, bonding and testing can be open-ended but should take 3months realistically. This gives a development iteration cycle time of 9months. At least 2 iterations should be expected with the new developments proposed. Then there will be extensive tests with the full system to confirm resolutions, radiation hardness and lifetime tests of bonded structure.

### 6.2 Electronics

Many of the basic blocks are available at RAL which allows a compact design cycle. These are unfortunately in non radiation-hard 0.7um and 0.5um technologies. If we trial some prototypes in these technologies it will take 6 effort months of design. This could be reduced to a 4 month period with two designers. Fabrication takes 3 months and testing will take 3 months.

We then move to the 0.25um processes to give us the radiation hardness and density for the final design. This will take 2months to create the design environments for our new structures. It will then take 6months to port the designs and re-simulate in the new technology. Again this could be done with 2 designers probably in a 3 months period. Then there is 3 months fabrication and 3 months test. We would have to allow for 2 iteration cycles.

It would be feasible to go straight to the 0.25um technology but in this case we would have to add a full iteration time to test out the initial ideas and to allow for the inevitable learning experiences.

### 7.0 Interconnection technology

We will use the low-temperature Gold Stud bump bonding technique, which will have to be Qualified for space applications. Indium bonding will probably involve too much risk in this potentially hot environment. Solder bonding may be a worth while alternative if it can be done without leaving too much built in stress in the detector. This might be a particular issue for the thinner detectors.

### 8.0 Future work

RAL ID is currently in discussion with Canberra about thin window detectors for low energy applications. It would be good to procure some thin window detectors from Canberra to test the ideas of n+ on n- pixellated detectors for this application. If this work is to go ahead with Canberra, funds will be needed as this is not in their development road-map for standard products.

RAL ID has an MSc student from Kings College London who will spend 6 months at RAL (starting at Easter) working on Silicon detectors for low-energy X-ray detection. This will involve measurements of existing Silicon Detector test structures to confirm capacitance, leakage current and low energy acceptance data. In addition to this a Case student is also going to spend some time at RAL on similar work but focussing on GaAs and 3D detectors.

Glasgow University is making measurements with existing RAL chips using a new 3D detector material. At present this is targeted at high-energy detection but with development these could also be an interesting technology for thin window low-energy detection. At present the development might be outside the time-scale of this project but we will track progress.

ID submitted a CFI bid to do pixellated high-energy detection. This would have involved a new pixel chip that could well be important for the development of this low-energy detection. This funding was not approved but is under appeal at present.

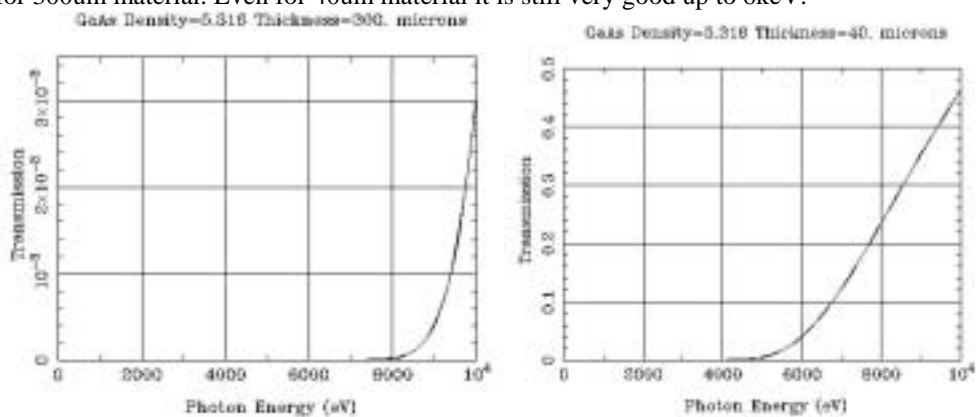
This work needs pump-priming funds for both the detector and electronics or it will not develop to a state where we could present a totally assured instrument development program.

### 9.0 Use of GaAs as the conversion material in place of Silicon

GaAs has a similar conversion mechanism as well as many parameters like band-gap (1.42eV) and Fano Factor (about 0.12 to 0.18), to that of Silicon. The major advantages are in X-ray absorption length, radiation damage tolerance. The potential disadvantages are leakage current and low-energy performance. The most recent and relevant paper on the subject from ESTEC [29] shows a significant improvement of the material and performance over other published data.

#### 9.1 High energy cut-off

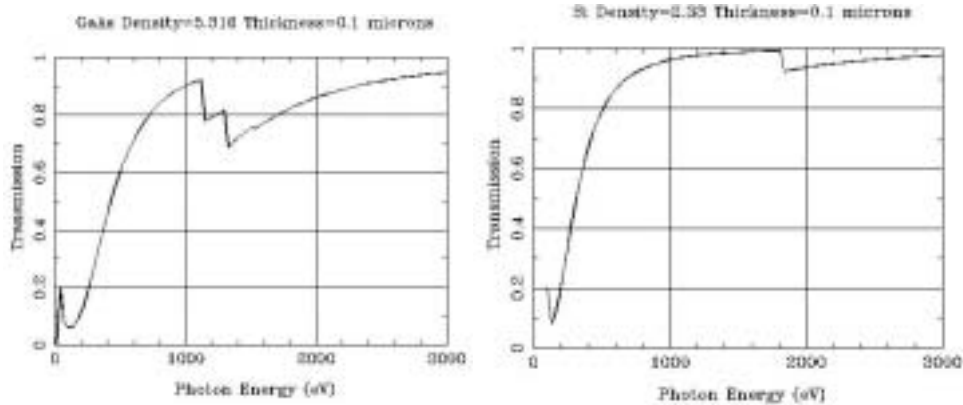
GaAs has a much higher average Z. This gives it a much greater stopping power as shown in the graph for 300um material. Even for 40um material it is still very good up to 6keV.



GaAs is clearly superior to silicon in this respect.

#### 9.2 Low energy cut-off

Detailed low energy X-ray data from GaAs detectors has not been seen but we might assume there is an inefficient layer near the metallic window side contacts. If this were to be 100nm to compare with the best silicon case we see the following efficiencies.



Clearly this is worse for GaAs but is acceptable, particularly if this dead region could be reduced. The metallic contacts on this surface are a mixture of Ti/Pi/Au but these are very thin and probably do not seriously affect performance.

At present the ESTEC 32x32 array has a 200um thick semi-insulating substrate on the window side for the Ohmic contact. This would obviously need to be completely removed and then the metallic contact placed on the epi-layer. They measured 250eV FWHM at 5.9keV, irradiating through the pixel side. They had a substantial low-energy continuum due to the 6um p+ pixel layer which would be reduced with a good Ohmic window.

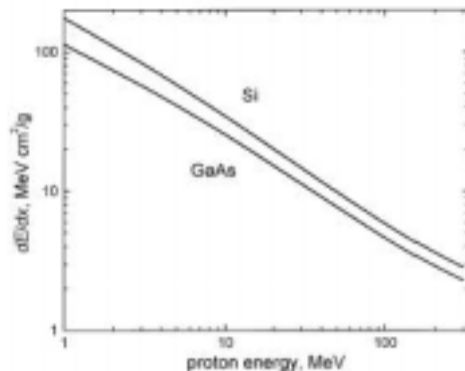
### 9.3 Leakage current

The ESTEC 32x32 array gives leakage currents of 3.5pA-10pA for a 300um square pixel on a 325um thick epi-layer material measured at room temperature with 50V bias. These also gave a very good measured inter-pixel resistance of 7e12Ohms. The array would perform very well with the electronics suggested in the rest of this paper and even better if a thinner layer was used to reduce leakage current. The electronics which is currently being built and is proposed for this GaAs detector is slightly different than defined here. It is intended for high leakage currents and dissipates 500uW/pixel for a total dissipation of 5W for 10000 pixels to give the 30mm x 30mm detector area.

### 9.4 Radiation hardness

This is probably the area where GaAs has its primary advantage over Si for a low-energy X-ray instrument. There are many references to GaAs detectors on semi-insulating material operating with marginal increases in leakage currents of charge collection efficiencies after many Mrad of ionising radiation and 10e13p/cm<sup>2</sup> [30], [31], Trobka [32].

This is due to decreased damage rather than cross-section as protons stop with very similar cross-section.



### 10.0 Overall conclusion and risk analysis

Overall the development of a 3cm x 3cm focal plane for X-ray spectroscopy with below 250eV resolution seems feasible with the Silicon technology proposed. The major development work centres on the thin window side layer for the detector and the low threshold measurement for the electronics. The noise in the detector and the electronics looks to be quite readily achieved. Both the developments identified above will require at least two iterations.

The primary concern is the silicon detector damage after proton irradiation. If the numbers presented (section 4.2.4.1) are representative of the environment around Mercury then the Silicon detector will require adequate shielding including the front side of the detector. This level of shielding might be unacceptable.

The alternative instrument based on a GaAs detector looks very promising if the semi-insulating layer can be substantially removed down to a thickness of a few hundred nanometers to achieve the low energy performance. A private communication suggests ESTEC group have a plan to take the energy resolution down to 500eV. A major advantage in this environment is the high tolerance to proton irradiation. The current best epi-layer material appears to be available only to the ESTEC group at present.

### 11.0 Acknowledgements

Thank you to R. Emery for arranging financial support from RAL SSTD to carry out the study. Thank you to Manuel Grande, Sarah Dunkin, Bruce Swinyard, Mark Prydderch and Marcus French for comments and technical input to the document.

### 13.0 References

1. Lechner, NIM A 377 (1996) p206
2. Surface barrier detectors using aluminium on n-and p-type silicon for alpha-spectroscopy NIM A 459(2001) p200
3. Experimental results of the response of semiconductor detectors to low energy photons. NIM A 439 (2000) p 239
4. Struder, NIM A 454 (2000) p73], [NIM A 439(2000) p216
5. NIM A 439 (2000) p567], [NIM A 377 (1996) p191
6. NIM A 439 (2000) p582
7. SPIE Vol. 3765 p285
8. NIM A 387 (1997) p250
9. B.L. Henke, E.M. Gullikson, and J.C. Davis. *X-ray interactions: photoabsorption, scattering, transmission, and reflection at E=50-30000 eV, Z=1-92*, Atomic Data and Nuclear Data Tables Vol. **54** (no.2), 181-342 (July 1993).
10. A Quantitative explanation of low energy tailing features of Si(Li) and Ge X-ray detectors.. NIM A 418 (1998) p394
11. An Analytical description of low energy X-ray spectra in Si(Li) and HPGe detectors. NIM A 439 (2000) p247
12. NIM A 439 (2000) p 319
13. NIM A 434 (1999) p82
14. NIM A 454 (2000) p73
15. ESA report on Smart 1 Shielding, S1-EST-RP-5025
16. IEEE Trans Nucl Sci Vol. 47, No.6 Dec 2000
17. NIM A 460 (2001) p336
18. NIM A 465 (2001) p70
19. IEEE Trans on NS Vol. 46 No4, (1999) p886
20. IEEE Trans on Nucl Sci Vol 45, No 2 , 1998 p186
21. NIM A 326 (1993) p3
22. IEEE Trans on NS Vol. 48, No 3. (2001) P493
23. IEEE Trans on NS Vol. 46, No 4. (1999) p 886
24. NIM A 395 (1997) p452
25. NIM A 390 (1997) p241
26. NIM A 409 (1998) p315
27. IEEE Trans on NS Vol. 47, No 3. (2000) p806
28. Summary of thermal, shot and flicker noise in detectors and readout, NIM A 426 (1999) p 538
29. Hard X-ray test and evaluation of a prototype 32x32 pixel GaAs array C. Erd, A. Owens et al. Eslab 2002/019/ST, EESTEC to be published in NIM A
30. IEEE Trans.Nucl.Sci. 44 (1997) 1705-1707
31. Radiation Physics and Chemistry Vol. 62 Issue 4. Oct 2001 p301
32. NIM A Vol 428 Issue 1 (1999) p199